Surface-enhanced circular dichroism spectroscopy mediated by nonchiral nanoantennas

Aitzol García-Etxarri and Jennifer A. Dionne

Phys. Rev. B **87**, 235409 — Published 10 June 2013

DOI: 10.1103/PhysRevB.87.235409

Surface enhanced circular dichroism spectroscopy mediated by non-chiral nanoantennas

Aitzol García-Etxarri[1] and Jennifer A. Dionne[1]

[1] *Department of Materials Science and Engineering, Stanford University, Stanford, California 94305, United States**

(Dated: April 18, 2013)

We theoretically investigate light-matter interactions for chiral molecules in the presence of non-chiral nanoantennas. Isotropic nanostructures supporting optical-frequency electric or magnetic dipoles are sufficient to locally enhance the excitation of a molecule's chiral polarizability and thus its circular dichroism spectrum. However, simultaneous electric and magnetic dipoles are necessary to achieve a net, spatially-averaged enhancement. Our contribution provides a theoretical framework to understand chiral light-matter interactions at the nanoscale and sets the necessary and sufficient conditions to enhance circular dichroism spectroscopy in the presence of nanoantennas. The results may lead to new, field-enhanced, chiral spectroscopic techniques.

PACS numbers: 78.30.-j, 33.70.-w, 73.22.Lp, 84.40.Ba

I. INTRODUCTION

Chiral objects - those whose mirror images are not superimposable - abound in nature. Examples range from spiral galaxies to human hands to nucleic acids. Chirality is fundamental to many biological, chemical, and physical processes: it can contribute to the gene flow and evolution of snail colonies[1], determine the effectiveness of pharmaceutical drugs, and impact the formation of fermionic condensates and superfluids. Nature's preference for a certain chirality, e.g. the fact that all proteins form a left-handed spiral while sugars twist to the right, constitutes one of life's greatest mysteries[2].

In electromagnetism, circularly-polarized light (CPL) is the paradigmatic example of a chiral field. Propagating in a dispersion-less medium, the electric and magnetic fields of CPL undergo one full rotation per period and wavelength. This rotation can be either clockwise or counter-clockwise. The spatial trajectories of these two waves form a chiral set of solutions to Maxwell's equations.

Circularly polarized light can be used to probe the geometric and electromagnetic chiral properties of molecules. A specific enantiomer of a chiral molecule will exhibit a preferential absorption of right or left-handed circularly polarized light. Circular dichroism (CD) spectroscopy measures this differential absorption in the ultraviolet and visible spectrum, while vibrational circular dichroism (VCD) extends the technique to the infrared[3]. Both CD and VCD are highly valuable techniques: for example, in molecular biology, they elucidate a protein's secondary structure, which in turn provides insight into the protein's function. In pharmacology, these techniques determine the chiral purity of chemical products and the absolute structure of pure enantiomers[4,5].

Despite the wide applicability of CD and VCD, their sensitivity is limited. Proteins and nucleic acids exhibit a differential absorption of left and right circularly polarized light which is nearly five orders of magnitude less than their absorption of unpolarized light. Hence, in order to get measurable signals, large sample concentrations or signal amplifiers are needed. This prohibits CD and VCD spectroscopy from entering the few molecule regime.

In recent years, engineered light-matter interactions at the nanoscale have enhanced the sensitivity of other spectroscopic techniques such as Surface Enhanced Raman Spectroscopy (SERS) and Surface-Enhanced Infra-Red Absorption spectroscopy (SEIRA). Nanostructured surfaces and nanoparticles supporting strong optical-frequency electric resonances have allowed SERS and SEIRA to reach single molecule and attomolar sensitivity, respectively[6–9]. In this paper, drawing on insights from SERS and SEIRA, we investigate the fundamental electromagnetic conditions necessary to increase the sensitivity of CD and VCD spectroscopy. Since chiral molecules are characterized by electric and magnetic dipoles, enhancing (V)CD spectroscopy requires control over both the electric *and* magnetic fields of light. Accordingly, attention is given to nanostructures supporting either electric *or* magnetic resonances, or both. We show that molecules near an electrically- or magnetically-resonant nanoparticle will experience a local, position-dependent chiral enhancement. Averaged over all space, such electrically- or magnetically-resonant nanoparticles do not produce a net enhancement of the (V)CD signal. In contrast, engineered nanostructures with combined electric and magnetic resonances do produce a global enhancement of the signal. Our results determine the necessary and sufficient conditions required to enhance chiral light-matter interactions, and may enable new spectroscopic techniques such as field enhanced circular dichroism or field enhanced vibrational circular dichroism.

II. THEORETICAL FORMALISM

To describe the excitation of chiral molecules by electric and magnetic fields of arbitrary polarization states, we adopt the formalism introduced by Tang and Cohen[10,11]. In general, we assume that a circularly polarized plane wave illuminates a nanoparticle, and that fields of arbitrary polarization will be generated in the surroundings of the particle. The rate of excitation of a randomly oriented chiral molecule illuminated by these fields can be expressed as:

$$A^{\pm} = \frac{1}{\varepsilon_0}\omega U_e^{\pm}\alpha'' + \mu_0\omega U_m^{\pm}\chi'' + \frac{2}{\varepsilon_0}C^{\pm}G'' \qquad (1)$$

where the plus and minus superscripts denote whether the fields originated from left- or right-handed circularly polarized incident light, respectively. $U_e^{\pm} = \frac{\varepsilon_0}{2}|\mathbf{E}^{\pm}|^2$ and $U_m^{\pm} = \frac{1}{2\mu_0}|\mathbf{B}^{\pm}|^2$ are the electric and magnetic energy densities respectively, α'' is the imaginary part of the electric polarizability, χ'' is the imaginary part of the magnetic susceptibility, and G'' is the imaginary part of the isotropic mixed electric-magnetic dipole (i.e., chiral) polarizability. As usual, ω, ε_0, and μ_0 denote the angular frequency of light and the permittivity and permeability of free space. $C^{\pm}$ denotes the electromagnetic density of chirality and can be defined as[10,12]:

$$C^{\pm} = \frac{1}{2c^2}\omega Im(\mathbf{E}^{*\pm}\cdot\mathbf{H}^{\pm}) = \frac{\varepsilon_0}{2}\omega|\mathbf{E}^{\pm}||\mathbf{H}^{\pm}|cos(\beta_{i\mathbf{E}^{\pm},\mathbf{H}^{\pm}}). \qquad (2)$$

In the above expression, $\beta_{i\mathbf{E},\mathbf{H}}$ denotes the angle between the complex $\mathbf{E}$ vector multiplied by the complex number i and the $\mathbf{H}$ vector.

The three terms of Eq. 1 account for molecular absorption due to electronic excitations of electric, magnetic, and chiral character respectively. For most molecules, χ is negligible, and the second term in Eq. 1 can be neglected. In this paper, we focus on techniques to enhance the third term, proportional to C, corresponding to chiral light-molecule interactions.

For circularly polarized light traveling in vacuum, $C_{cpl} = \pm\frac{\varepsilon_0\omega}{c}E_0^2$ where E_0 is the incoming electric field amplitude. Such propagating solutions of Maxwell's equations satisfy $cos(\beta_{i\mathbf{E},\mathbf{H}}) = \pm 1$, indicating, as recently pointed out by others[12–14], that CPL is an optimum polarization state to maximize the excitation rate of chiral transitions in chiral molecules. However, Eq. 2 shows that it is possible to enhance chiral light-matter interactions by enhancing the electric and/or magnetic fields, provided their polarization state and relative phase remain approximatively unaltered.

Since CD measures the differential absorption of a system excited by right and left-handed CPL, the measured signal can be expressed as

$$CD \propto A^+ - A^- = \frac{\omega}{\varepsilon_0}\alpha''(U_e^+ - U_e^-) + \frac{2}{\varepsilon_0}G''(C^+ - C^-). \qquad (3)$$

C is an electromagnetic pseudo scalar (it flips sign under parity), while U_e instead is a pure scalar (it does not flip its sign)[10,11]. Accordingly, for circularly polarized light, $CD_{cpl} = \frac{4}{\varepsilon_0}G''|C_{cpl}|$. As seen, the measured signal is proportional to the chiral polarizability of the molecule (G), allowing CD techniques to unveil the chiral electromagnetic properties of molecules.

In this letter, we investigate this process in the presence of isotropic, non-chiral nanoantennas. Due to the isotropic nature of the antenna, a parity inversion on the system composed of the particle and incident fields will exclusively change the handedness of the incident fields. Consequently, exciting the antenna with left and right CPL will be equivalent to applying a parity operation over the system. Moreover, due to the symmetry properties of C and U_e, the electromagnetic fields in the presence of an achiral antenna at an arbitrary position will hold the following properties: $C^+ = C = -C^-$ and $U_e^+ = U_e^-$. Since the polarizability of a molecule is much smaller than the polarizability of a typical optical antenna, the presence of the molecule will not significantly perturb the optical response of the antenna. Under these assumptions, Eq. 3 can be simplified to

$$CD \propto A^+ - A^- = \frac{4}{\varepsilon_0}G''C. \qquad (4)$$

Eq. 4 can be rewritten as $CD = fCD_{cpl}$, where $f = \frac{C}{|C_{cpl}|}$. In the presence of an antenna, this is a position dependent quantity. Hence, from now on we will refer to this quantity as the local CD enhancement factor $f(\mathbf{r})$. Note that if the antenna were by any means chiral[15], the the parity relations for C and U_e would not be fulfilled and Eq. 4 would not be valid to describe CD spectroscopy in the presence of a particular nanoantenna.

Can a nanoparticle enhance CD spectroscopy? Recent circular dichroism studies performed on molecules in the presence of chiral[14,16–19] and plasmonic nanostructures[20–27] suggest that the approach has potential. However, a fundamental understanding of these processes is still lacking.

III. ELECTRIC OR MAGNETIC DIPOLAR ANTENNAS

Let us start by considering the optical response of a small plasmonic nanoparticle. If the size of the nanoparticle is much smaller than the wavelength of light, the electrostatic approximation holds and the response of the sphere can be modeled as an electric dipole. Assuming that the particle is illuminated by a plane wave of arbitrary polarization, the sphere will acquire an electric dipolar moment $\mathbf{p}_e = \alpha_e\mathbf{E_{inc}}$, where $\mathbf{E_{inc}}$ is the incoming electric field vector, $\alpha_e = 4\pi\varepsilon_0 a^3\frac{\varepsilon-1}{\varepsilon+2}$ is the electric polarizability of the sphere in vacuum, ε is the permittivity of the particle, and a is the radius of the sphere.

In the near-field of the electrically-resonant nanoparticle, the total fields can be expressed as the sum of scat-

tered and incoming fields. Since the magnetic near fields scattered by an electric dipole are negligible in the electrostatic limit, we find:

$$\mathbf{E_{tot}} = \mathbf{E_{scat}} + \mathbf{E_{inc}} = \frac{k^2}{\varepsilon_0}\mathbf{G_e p_e} + \mathbf{E_{inc}} \tag{5}$$

$$\mathbf{H_{tot}} = \mathbf{H_{scat}} + \mathbf{H_{inc}} \approx \mathbf{H_{inc}}, \tag{6}$$

where k is the wavenumber in vacuum and $\mathbf{E_{scat}}$, $\mathbf{H_{scat}}$, and $\mathbf{H_{inc}}$ are the scattered and incident electric and magnetic field vectors. $\mathbf{G_e}$ is the electric dyadic Green's tensor in the near field limit, given by reference[28]. For simplicity, we assume that the sphere is located at the origin of coordinates ($\mathbf{r_0} = 0$) and is illuminated by a plane wave traveling in the positive $\hat{z}$ direction.

For circularly polarized illumination, the local density of chirality C in the near field of the sphere can be analytically calculated by substituting Eqs.5 and 6 into Eq. 2. The resulting expression for the position dependent CD enhancement is given in Table I as $f^{\alpha_e}(\mathbf{r})$.

As an example, consider the response of a 10 nm radius silver sphere, determined by rigorously solving Maxwell's equations using the Boundary Element Method (BEM)[29,30]. Fig.1a plots the extinction cross section of the sphere, as well as the position-dependent CD enhancement factor, $f(\mathbf{r})$, calculated at a point 1 nm above the particle, and the average enhancement, defined as the local enhancement integrated over a surface, normalized to the surface area: $f_{avg} = \int f(\mathbf{r})dS/(4\pi r^2)$. As seen, the localized surface plasmon resonance occurs at a wavelength of $\lambda = 355$ nm, where the extinction cross-section is maximum. Here, the absolute value of the density of chirality is minimized. Since the electric dipole is on-resonance, the phase of $\mathbf{E_{scat}}$ will be $\pi/2$ delayed with respect to the incoming magnetic field. Therefore, the phase of the total (incident and scattered) fields results in $cos(\beta_{i\mathbf{E},\mathbf{H}}) \approx 0$ and, consequently, according to Eq. 2, $f \propto C \approx 0$.

Slightly off the plasmonic resonance, however, the ideal phase relation between the electric and magnetic field is not completely destroyed, and a local enhancement of $f(\mathbf{r})$ can be obtained. Fig.1b and c show the total electric field enhancement and the CD enhancement factor $f(\mathbf{r})$, plotted along a spherical surface 1 nm away from the particle for $\lambda = 359$ nm, red-shifted slightly from the plasmon resonance of $\lambda = 355$ nm. As seen, $f(\mathbf{r})$ is both positively and negatively enhanced in different regions around the nanoparticle. Here, a negative enhancement of $f(\mathbf{r})$ indicates that a left-handed excitation will induce right-handed near fields. Positive-enhanced values of $f(\mathbf{r})$ imply that the chirality will be increased while the handedness of the fields will remain unchanged.

Neglecting retardation of the incident electromagnetic fields in the vicinity of the particle, the analytic average density of CD enhancement is found to be $f_{avg} = 1$. Fig.1a (red line) plots this averaged CD enhancement factor for the fully electrodynamically calculated fields

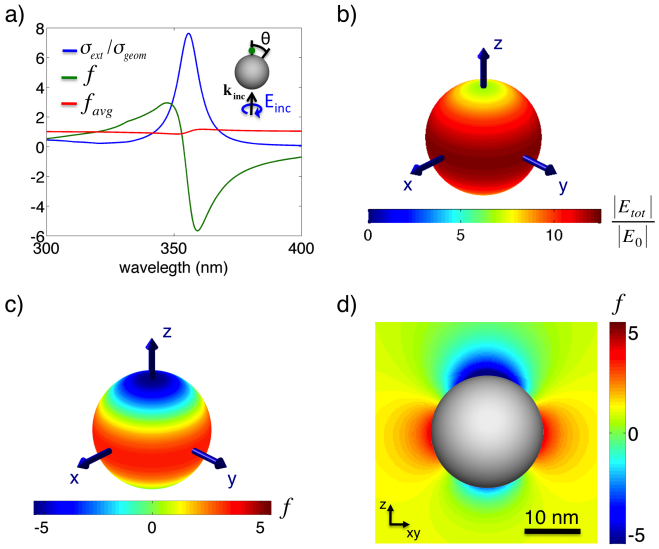

FIG. 1. 10 nm radius silver nano sphere illuminated by a circularly polarized plane wave. a) Spectral response of the nanostructure. Blue: geometrically normalized extinction cross section. Green: CD enhancement factor, $f(\mathbf{r})$, 1 nm on top of the sphere (green dot in the inset). Red: CD enhancement factor averaged over a sphere covering the particle (f_{avg}). b) Total electric near field amplitude enhancement at the plasmonic resonance ($\lambda = 359$ nm) plotted over a surface 1 nm above the nanoparticle. c) CD enhancement factor, $f(\mathbf{r})$, at that same surface and wavelength. d) $f(\mathbf{r})$ for the same wavelength plotted over a plane crossing the sphere and the incident wavevector.

around the particle. The small deviations from the predicted analytical value of 1 are due to retardation effects.Therefore, a plasmonic nanoparticle illuminated by circularly polarized light will not enhance CD spectroscopy if isotropically surrounded by chiral molecules. However, surface-enhanced CD spectroscopy could be achieved by creating a surface of closely-packed nanoparticles, where molecules are prohibited from laying in regions of opposite $f(\mathbf{r})$. The specifics of the design of such a surface will be left for future work.

Now consider an ideal optical-frequency magnetic dipole illuminated by CPL. Expressions for the CD enhancement factor are included in Table I as $f^{\alpha_m}(\mathbf{r})$. As with electric dipoles, local enhancement of $f(\mathbf{r})$ is possible, but averaging the CD enhancement factor on a sphere of constant radius yields no net enhancement.

IV. SIMULTANEOUS ELECTRIC AND A MAGNETIC DIPOLAR ANTENNAS

The previously described situation is significantly modified when considering a combination of an isotropic electric and an isotropic magnetic dipole. If the dipoles are located at the same spatial position, symmetry dictates that they will not interact; accordingly bi-anisotropy will not be generated[31]. In the electrostatic limit, assuming

	$f(\mathbf{r}) = \frac{C(\mathbf{r})}{C_{cpl}}$
α_e	$f^{\alpha_e}(\mathbf{r}) = \pm\left[1 + \frac{1}{2}\frac{1}{4\pi\varepsilon_0}\frac{1}{r^3}(1-3cos^2\theta)\lvert\alpha_e\rvert cos(\varphi_e)\right]$
α_m	$f^{\alpha_m}(\mathbf{r}) = \pm\left[1 + \frac{1}{2}\frac{1}{4\pi}\frac{1}{r^3}(1-3cos^2\theta)\lvert\alpha_m\rvert cos(\varphi_m)\right]$
$\alpha_e + \alpha_m$	$f^{\alpha_e+\alpha_m}(\mathbf{r}) = f^{\alpha_e}(\mathbf{r}) + f^{\alpha_m}(\mathbf{r}) \pm \left[-1 + \frac{1}{2}\frac{1}{4\pi\varepsilon_0}\frac{1}{4\pi}\frac{1}{r^6}(5-3cos^2\theta)\lvert\alpha_e\rvert\lvert\alpha_m\rvert cos(\varphi_m-\varphi_e)\right]$

TABLE I. Analytic expressions for the position dependent CD enhancement factor $f(\mathbf{r})$ around different basic electromagnetic modes. α_e and α_m account for an electric and a magnetic polarizability respectively. φ_e and φ_m represent the phase of α_e and α_m respectively. θ is the spatial elevation angle (see inset in Fig.1a).

that the magnetic fields produced by an electric dipole as well as the electric fields produced by a magnetic dipole are negligible, the total near fields produced by such a system can be approximated as:

$$\mathbf{E_{tot}} = \mathbf{E_{scat}} + \mathbf{E_{inc}} \approx \frac{k^2}{\varepsilon_0}\mathbf{G_e p_e} + \mathbf{E_{inc}} \tag{7}$$

$$\mathbf{H_{tot}} = \mathbf{H_{scat}} + \mathbf{H_{inc}} \approx k^2\mathbf{G_e p_m} + \mathbf{H_{inc}}, \tag{8}$$

For circularly polarized incident light, averaging the position dependent $f(\mathbf{r})$ ($f^{\alpha_e+\alpha_m}(\mathbf{r})$ in Table I) gives the following expression:

$$f_{avg}^{\alpha_e+\alpha_m} = \left[1 + \frac{1}{4\pi\varepsilon_0}\frac{1}{2\pi}\frac{1}{r^6}\lvert\alpha_e\rvert\lvert\alpha_m\rvert cos\left(\varphi_m - \varphi_e\right)\right] \tag{9}$$

which in general can be greater than 1. φ_m and φ_e account for the phase of the magnetic and electric polarizability, respectively.

While optical-frequency magnetic dipoles are uncommon in nature, recently-engineered nanostructures can exhibit strong electric and magnetic resonances at visible and near-infrared frequencies. Examples include split-ring resonators, nanocups or nanocrescents[32–34], as well as rings of metallic nanoparticles[35]. As an example of a system showing isotropic electric and magnetic resonances, we consider a spherical silicon nanoparticle[36–39]. Due to their high refractive index, these particles support electric and magnetic Mie resonances in the visible and infrared part of the spectrum[36].

The upper panel of Fig.2a shows the geometrically normalized extinction cross section of a 75 nm radius Si nanoparticle, calculated using the BEM. In order to analyze the electromagnetic nature of the different emerging resonances, we performed a Mie calculation on the same system and calculated the contribution of the lowest order electric and magnetic terms in the Mie series to the total extinction spectrum[40]. The lowest energy peak, as expected for a high index nanoparticle[36], corresponds to the magnetic dipole term b_1 in the Mie expansion and can be associated with the magnetic polarizability through $\alpha_m = \frac{i}{\mu_0}\left(\frac{k^3}{6\pi}\right)^{-1} b_1$. The second peak instead is associated with the electric dipolar term in the expansion, a_1. Correspondingly, one can calculate the electric polarizability associated to this term as $\alpha_m = i\varepsilon_0\left(\frac{k^3}{6\pi}\right)^{-1} a_1$. The contributions of these to modes to

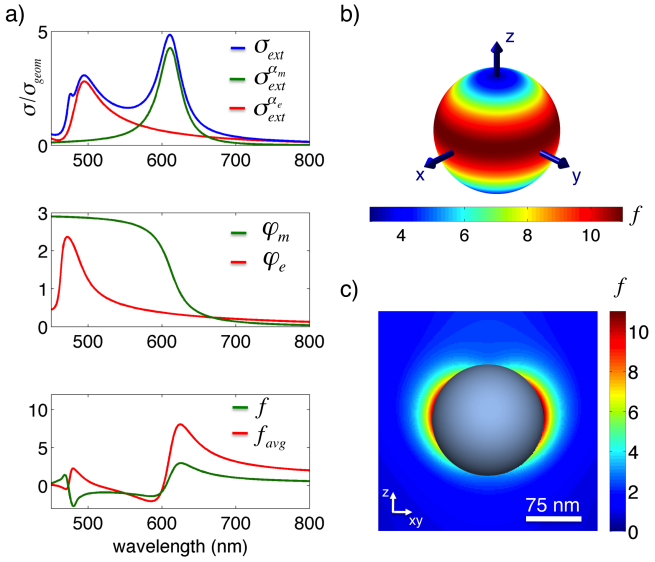

FIG. 2. 75 nm radius silicon nanosphere illuminated by circularly polarized light. a) Upper panel: The geometrically normalized extinction cross section is plotted in blue. Green and red lines plot the magnetic and electric dipolar contributions to the total extinction cross section respectively. Middle panel: phase behavior of the magnetic (green) and electric (red) dipolar contributions. Lower panel: CD enhancement factor $f(\mathbf{r})$ at a position 1nm on top of the sphere and averaged CD enhancement f_{avg} plotted in green and red respectively. The spatially averaged CD enhancement factor is enhanced in the spectral regions where $cos(\varphi_m - \varphi_e) \sim \pm 1$. b) CD enhancement factor at a surface covering the nanoparticle for a separation distance of 1 nm at $\lambda = 625nm$. c) CD enhancement factor for the same wavelength plotted over a plane crossing the sphere.

the geometrically normalized total extinction cross section can be then calculated as $\sigma_{ext}^{\alpha_m} = \frac{1}{\pi a^2} kIm(\alpha_m)$ and $\sigma_{ext}^{\alpha_e} = \frac{1}{\pi a^2} kIm(\alpha_e)$[36]. The middle panel illustrates the phase behavior of the polarizabilities α_e and α_m. According to Eq. 9, the averaged chiral density will be increased only if $cos(\varphi_e - \varphi_m) \sim \pm 1$ while $|\alpha_e|$ and $|\alpha_m|$ are still considerably large, a condition which is satisfied in the green and red wavelength regions of the visible spectrum. The lower panel plots the local chiral density at a point 1 nm above the nanoparticle (green) and the averaged chiral density (red) around the particle. As seen, unlike an isolated electric or magnetic dipole, the total averaged

chiral density is enhanced compared to CPL.

Fig.2b and c plot the three-dimensional surface (1 nm above the sphere) and two-dimensional cross-section of $f(\mathbf{r})$ for $\lambda = 625$ nm. At this wavelength, the maximum local and averaged CD enhancement factor occur. Remarkably, $f(\mathbf{r})$ is exclusively positive throughout all space at this wavelength. Moreover, the averaged enhancement factor exceeds that of circularly polarized light by nearly an order of magnitude. In other words, solution-based CD spectroscopy can be enhanced globally via isotropic achiral nanostructures supporting electric and magnetic dipoles.

V. CONCLUSIONS AND OUTLOOK

In conclusion, we have shown how individual electric or magnetic dipoles can tailor the local density of chirality and thus the circular dichroism enhancement. Individual electric or magnetic dipoles can only locally (but not globally) increase the CD enhancement factor. Consequently, they could be used to increase the sensitivity of surface-based circular dichroism techniques, but are ill-suited for solution-phase measurements. In contrast, combinations of electric and magnetic dipoles can achieve both local and net, global enhancements of the CD signal, and are therefore strong candidates for solution-phase surface enhanced (V)CD. Si nanoparticles, for example, increase the averaged CD enhancement factor by nearly a factor of ten. Further engineering of the electric and magnetic response of nanoantennas may lead to much higher enhancement factors. Interestingly, we demonstrate that structurally chiral particles are not necessary to enhance CD spectroscopy. These results set a theoretical basis for field-enhanced circular dichroism spectroscopy, a valuable technique in fields ranging from molecular biology to pharmacology.

ACKNOWLEDGMENTS

We thank Sassan Sheikholeslami and Hadiseh Alaeian for insightful discussions and the Donostia International Physics Center (DIPC) for their computational resources. Funding from a NSF Career Award (DMR-1151231) and Stanford's Global Climate and Energy Project are gratefully acknowledged.

* aitzol@stanford.edu

[1] R. Ueshima and T. Asami, Nature **425**, 679 (2003).
[2] R. A. Hegstrom and D. K. Kondepudi, Scientific American **262**, 108 (1990).
[3] L. D. Barron, *Molecular Light Scattering and Optical Activity*, 2nd ed. (Cambridge University Press, 2004).
[4] A. Rodger, *Circular Dichroism and Linear Dichroism. Enciclopedia of Analytical Chemistry* (2006).
[5] P. L. Polavarapu and C. Zhao, Fresenius' Journal of Analytical Chemistry **366**, 727 (2000).
[6] S. Nie and S. R. Emory, Science **275**, 1102 (1997).
[7] K. Kneipp, Y. Wang, H. Kneipp, L. Perelman, I. Itzkan, R. Dasari, and M. Feld, PRL **78**, 1667 (1997).
[8] H. Xu, E. J. Bjerneld, M. Käll, and L. Börjesson, Physical Review Letters **83**, 4357 (1999).
[9] F. Neubrech, A. Pucci, T. Cornelius, S. Karim, A. Garcia-Etxarri, and J. Aizpurua, Physical Review Letters **101**, 157403 (2008).
[10] Y. Tang and A. E. Cohen, Physical Review Letters **104**, 163901 (2010).
[11] Y. Tang and A. E. Cohen, Science **332**, 333 (2011).
[12] K. Y. Bliokh and F. Nori, Physical Review A **83**, 021803 (2011).
[13] D. L. D. Andrews and M. M. M. Coles, Optics Letters **37**, 3009 (2012).
[14] E. Hendry, R. Mikhaylovskiy, L. Barron, M. Kadodwala, and T. J. Davis, Nano Letters **12**, 3640 (2012).
[15] E. Plum, V. A. Fedotov, and N. I. Zheludev, Journal of Optics A: Pure and Applied Optics **11**, 074009 (2009).
[16] E. Hendry, T. Carpy, J. Johnston, M. Popland, R. V. Mikhaylovskiy, A. J. Lapthorn, S. M. Kelly, L. D. Barron, N. Gadegaard, and M. Kadodwala, Nature Nanotechnology **5**, 783 (2010).
[17] V. V. Klimov, D. V. Guzatov, and M. Ducloy, Europhysics Letters **97**, 47004 (2012).
[18] D. Guzatov and V. Klimov, arXiv:1203.5393v1 (2012).
[19] M. Schäferling, D. Dregely, M. Hentschel, and H. Giessen, Physical Review X **2**, 031010 (2012).
[20] J. M. Slocik, A. O. Govorov, and R. R. Naik, Nano Letters **11**, 701 (2011).
[21] H. Zhang and A. O. Govorov, arXiv:1207.0150v1 (2012).
[22] A. O. Govorov, Z. Fan, P. Hernandez, J. M. Slocik, and R. R. Naik, Nano Letters **10**, 1374 (2010).
[23] A. O. Govorov, The Journal of Physical Chemistry C **115**, 7914 (2011).
[24] A. O. Govorov and Z. Fan, ChemPhysChem **13**, 2551 (2012).
[25] I. Lieberman, G. Shemer, G. Markovich, and 5, Angewandte Chemie (International Edition) **47**, 4855 (2008).
[26] M. Schäferling, X. Yin, and H. Giessen, Optics Express **20**, 26326 (2012).
[27] T. J. Davis and E. Hendry, Phys. Rev. B **87**, 085405 (2013).
[28] $\mathbf{G_e p} = \frac{1}{4\pi}\frac{e^{ikr}}{k^2 r^3}\left(3\mathbf{n}(\mathbf{n}\cdot\mathbf{p}) - \mathbf{p}\right)$, where $\mathbf{p}$ represents a generic dipolar moment (electric or magnetic), $r = |\mathbf{r} - \mathbf{r_0}|$ is the distance between the position of the dipole ($\mathbf{r_0}$) and the observation point $\mathbf{r}$, and $\mathbf{n}$ is the unit vector in the direction of $|\mathbf{r} - \mathbf{r_0}|$.
[29] F. de Abajo and A. Howie, Physical Review B **65**, 115418 (2002).
[30] F. G. de Abajo and A. Howie, Physical Review Letters **80**, 5180 (1998).
[31] S. N. Sheikholeslami, A. Garcia-Etxarri, and J. A. Dionne, Nano Letters **11**, 3927 (2011).
[32] Y. Zhang, A. Barhoumi, J. B. Lassiter, and N. J. Halas, Nano Letters **11**, 1838 (2011).

[33] A. Shevchenko and V. Ovchinnikov, Plasmonics **4**, 121 (2009).
[34] A. C. Atre, A. García-Etxarri, H. Alaeian, and J. A. Dionne, Advanced Optical Materials , http://dx.doi.org/10.1002/adom.201200022 (2013).
[35] V. N. Manoharan, P. Nordlander, G. Shvets, and F. Capasso, Science **328**, 1135 (2010).
[36] A. García-Etxarri, R. Gómez-Medina, L. S. Froufe-Pérez, C. López, L. Chantada, F. Scheffold, J. Aizpurua, M. Nieto-Vesperinas, and J. J. Sáenz, Optics Express **19**, 4815 (2011).
[37] A. B. Evlyukhin, S. M. Novikov, U. Zywietz, R. L. Eriksen, C. Reinhardt, S. I. Bozhevolnyi, and B. N. Chichkov, Nano Letters **12**, 3749 (2012).
[38] A. I. Kuznetsov, A. E. Miroshnichenko, Y. H. Fu, J. Zhang, and B. Luk'yanchuk, Scientific Reports **2**, (2012).
[39] M. Schmidt, R. Esteban, J. Sáenz, I. Suárez-Lacalle, S. Mackowski, and J. Aizpurua, Optics Express **20**, 13636 (2012).
[40] C. F. Bohren and D. R. Huffman, *Absorption and Scattering of Light by Small Particles* (Wiley-VCH, 2008).